Performance Analysis of Distance Protection in Presence of Type III Wind Turbine Generators

Ardavan Mohammadhassani, Nicholas Skoff, and Ali Mehrizi-Sani The Bradley Department of Electrical and Computer Engineering Virginia Polytechnic Institute and State University, Blacksburg, VA 24061 Email:{ardavanmh93, nms135, mehrizi}@vt.edu

Abstract—Type III wind turbine generators exhibit unconventional fault current behavior due to several reasons including the intermittent nature of wind energy, low-voltage ride through constraints, and their large slip variation. This behavior adversely affects the distance protection schemes on transmission lines adjacent to wind farms. This paper aims to investigate the performance of distance protection relays equipped with directional comparison blocking technology in the presence of Type III wind turbines. Studies are performed on the modified IEEE 9-bus system in PSCAD/EMTDC software to evaluate various scenarios.

Index Terms—Power system transients, power system faults, power system protection, wind power generation

I. INTRODUCTION

Wind energy has become an important source for electric power generation due to recent advancements in the field of power electronics and electric power generation technologies. According to the American Wind Energy Association, 7.2% of the electricity in the United States in 2019 was produced by wind energy which is enough to power 27.5 million homes. Moreover, as of the first quarter of 2020, there is 107,443 MW of wind generation capacity in the United States [1].

Currently, Type III wind turbines are a common choice for designing wind power generation systems [2], [3]. However, these particular machines are susceptible to converter and grid faults [4]–[6]. Meanwhile, the North American Electric Reliability Corporation (NERC) requires inverter-based generation units to remain connected during faults and to provide reactive power support as part of low voltage ride through (LVRT) [7]. This has led to various hardware- and software-based LVRT solutions for Type III wind turbines [8], [9]. However, LVRT implementations cause the fault current contribution of the wind turbines to be very small and unconventional. This can cause protection issues in transmission systems, where distance protection is the common choice.

Reference [10] analyzes the response of Type III wind turbines to three-phase faults in the transmission system and its effect on the performance of distance protection. This paper shows that Type III wind turbines exhibit fault currents at an off-nominal frequency during symmetrical faults. This is because these devices normally operate in a slip range of $\pm 30\%$. Therefore, the frequency of the fault current during symmetrical faults is between 42 Hz and 78 Hz for a 60 Hz system. This causes the phasor estimation of a digital protection relay to be inaccurate and potentially cause a

misoperation. The performance of distance protection in the presence of offshore wind farms connected through HVDC is investigated in [11]. This paper verifies that due to rapid reactive power control of the grid-side converter of the HVDC system, the backup distance protection relay might overestimate the fault distance. A μ -synthesis robust controller is designed to keep the current ratio constant and overcome this problem. Reference [12] proposes a method to analyze and improve the effect of wind intermittency on the performance of distribution system distance relays that use the concept of prefault memory voltage as polarizing quantities. An adaptive relay characteristic is proposed to account for wind intermittency caused by variations in penetration levels, wind speed, and distributed generation (DG) topology. An adaptive branch coefficient is proposed in [13] to make the zone 2 setting of the distance relay more adaptive to system conditions. This method can realize online detection and real-time calculation of settings according to fault type and sequence impedance of the wind turbine generator.

In spite of various methods being introduced in the literature for mitigating the effects of wind generation on distance protection, none of the aforementioned references consider directional comparison blocking (DCB) in distance relays. This method is commonly used for successful coordination of distance relays whenever there is a reverse fault in the system. This method relies on measuring the negative-sequence impedance, which makes it very robust since sequence currents are only large in magnitude for unbalanced conditions [14]. Additionally, the effect of the wind turbine LVRT system on the performance of distance protection is not discussed.

This paper analyzes the performance of a distance protection algorithm covering the line adjacent to a wind farm, while incorporating a sequence directionality element and the effect of the LVRT system. Several simulation case studies are investigated on the modified IEEE 9-bus system in PSCAD/EMTDC software. An evaluation is provided on the performance of distance relays with DCB in presence of Type III wind farms.

This paper is structured as follows: Section II provides a brief insight into the structure and control of Type III wind turbines. A short overview of distance relays with DCB is provided in Section III. Simulation results are provided and discussed in Section IV. Ultimately, conclusions are provided in Section V.

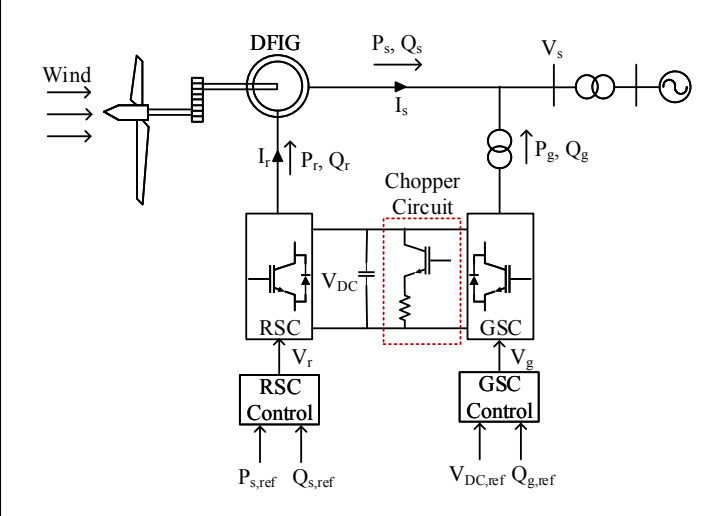


Fig. 1. Basic diagram of a Type III wind turbine.

II. TYPE III WIND TURBINE TECHNOLOGY

This section provides a brief insight into the Type III wind turbine model used in this paper [15].

A. Wind Power Model

The mechanical power extracted from the wind P_{mech} is calculated as

$$P_{mech} = \frac{1}{2} \rho A v_w^3 C_p(\lambda, \beta), \qquad (1)$$

where ρ is the density of air, A is the sweep area of the rotor in a wind turbine, v_w is the wind speed, C_p is the power coefficient, λ is the tip-speed ratio, and β is the pitch angle. The power coefficient is defined as $|\mathbf{V}_{s,\mathrm{ref}}|$

$$C_{p}(\lambda,\beta) = C_{1} \left(\frac{C_{2}}{\lambda_{i}} - C_{3}\beta - C_{4}\right) e^{-\frac{C_{5}}{\lambda_{i}}} + C_{6}\lambda$$

$$\frac{1}{\lambda_{i}} = \frac{1}{\lambda + 0.08\beta} - \frac{0.035}{\beta^{3} + 1}$$

$$C = [0.5176, 116, 0.4, 5, 21, 0.0068].$$
(2)

Maximum power point tracking (MPPT) is achieved using

$$P_{\text{MPPT}} = K_{\text{MPPT}} \omega_{rot}^3, \tag{3}$$

where P_{MPPT} is the maximum power point, K_{MPPT} is an optimal constant, and ω_{rot} is the rotor speed referred to the generator side of the gearbox [15].

B. Vector Control of the Wind Generator

Fig. 1 shows the basic diagram of the Type III wind turbine model. The grid-side converter (GSC) maintains the DC bus voltage V_{DC} while controlling the reactive power Q_g delivered or absorbed by the rotor. The rotor-side converter (RSC) controls the stator active power P_s and reactive power Q_s . A chopper circuit is employed in parallel with the DC bus for implementing LVRT. Fig. 2 shows the GSC control system. The voltages and currents are measured on the GSC side for decoupled control of V_{DC} and Q_g . V_{DC} is controlled via I_{gd} ,

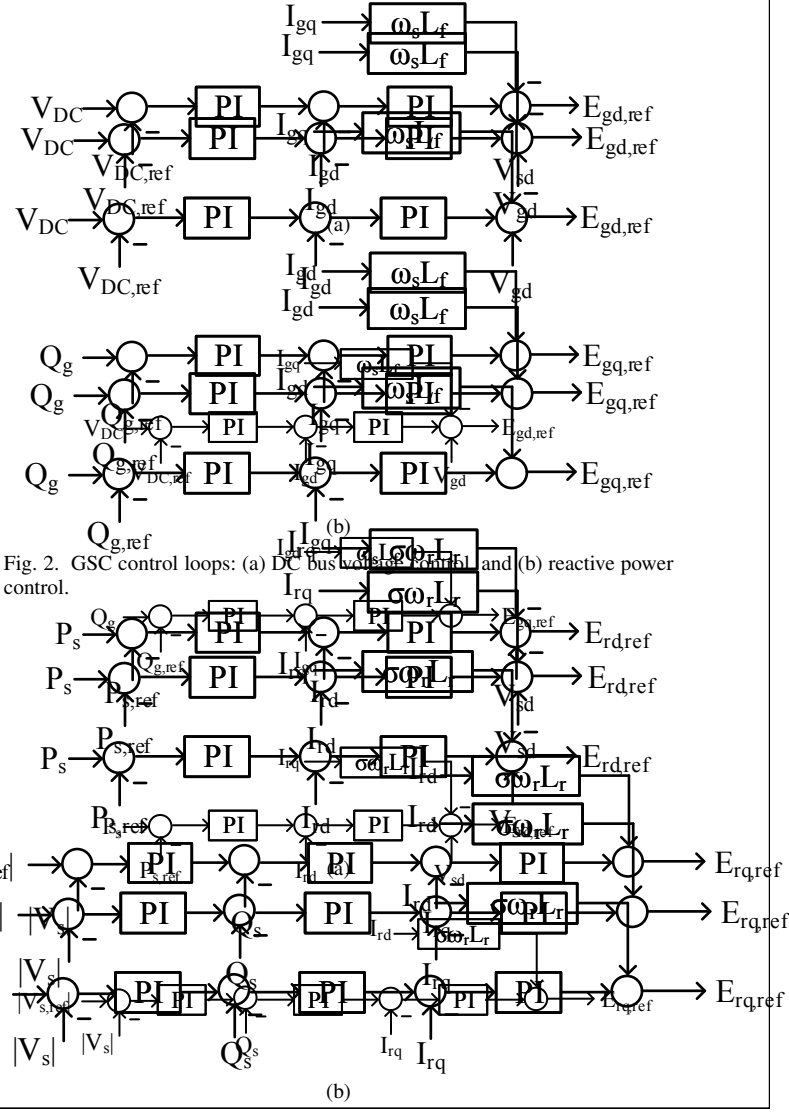


Fig. 3. RSC control loops: (a) stator active power control, and (b) stator reactive power control.

and Q_g is controlled via I_{gq} . Fig. 3 shows the control loops for the RSC. P_s is maintained at P_{MPPT} through controlling the d-axis component of the rotor current I_{rd} . Q_s , however, is controlled in proportion to the AC bus voltage. Controlling Q_s is achieved by controlling the q-axis component of the rotor current I_{rq} .

III. BASICS OF DISTANCE PROTECTION AND DIRECTIONAL COMPARISON BLOCKING

The protection scheme implemented in this paper is discussed within this section [14].

A. Zones of Protection and the Mho Circle

Distance protection schemes for transmission lines use the ratio between voltage and current phasors to determine if interruptive action is required. This is because the sensed impedance during steady state conditions is vastly different

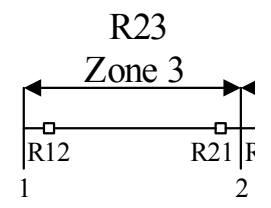


Fig. 4. 4-bus r

from that during a faul there are two zones c in the complex plane.

Fig. 4 shows a rarelay stations and zon midpoint of line 2-3. end of the line, showr in Fig. 5 represents t and bus 3. If the impedent in the instantaneous to the instantaneous

B. Directional Compa

Various methods ex but a popular one in components. Since se

large in magnitude for severcy unou makes them a robust way to characterinegative sequence values are immune tual coupling between parallel lines. Th sequence methods, making them less reapplications.

Consider a fault immediately in zo of measuring three-phase voltage and negative sequence impedance is -Z impedance behind the relay. For a faul measured quantity is instead $Z_{L2} + Z$ plus the remote source impedance. To tween these two sequence impedances,

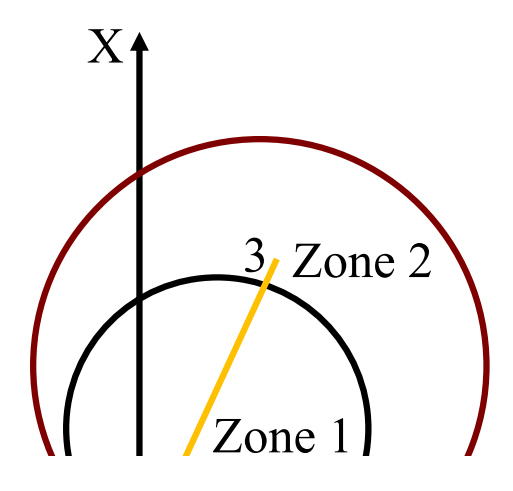
direction of the fault. Thresholds are selected that divide the complex plane into "forward" and "reverse" regions.

The negative sequence impedance plane is shown in Fig. 6. Impedances underneath the ZF line represent forward faults, and impedances above the ZR line are reverse. The threshold design method is formulated as

$$ZF = 0.5 \times Z_L$$

$$ZR = ZF + 0.1.$$
(4)

A common setting for the forward threshold is half of the line impedance. Then, the reverse threshold is calculated by adding 0.1 Ω to the previous result. Using these settings, an ample margin is provided between the thresholds and the ideal measured quantities.



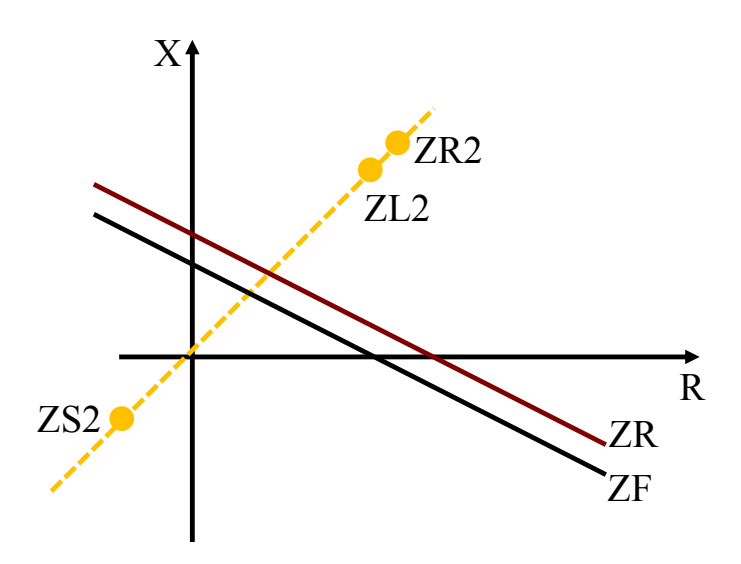


Fig. 6. Negative-sequence impedance thresholds.

IV. PERFORMANCE EVALUATION

A. Model Validation

The IEEE 9-bus system shown in Fig. 7 is modeled in PSCAD/EMTDC for performing simulations and studying different scenarios [16]. G₃ is replaced by an equivalent wind farm for performance evaluation. The wind farm is an aggregated model of 42 wind turbines, each having a 2.5MW rating [17]. Since the performance of distance relays protecting the line adjacent to the wind farm is to be studied, two circuit breakers are added to protect the line between bus 8 and bus 9. In order to validate the distance relay models built in PSCAD/EMTDC, a reverse line-to-ground (L-G) fault is simulated at bus 8. Fig. 8(a) shows the positive-sequence impedance trajectory at bus 9. As expected, the impedance trajectory settles in zone 2. As shown in Fig. 8(b),

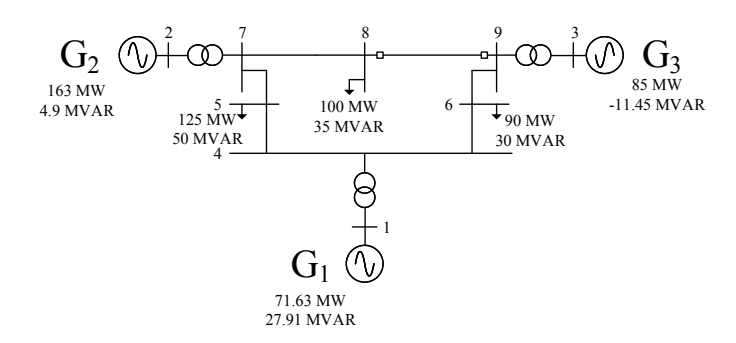


Fig. 7. The studied 9-bus system.

the negative-sequence impedance settles above the dashed red line, confirming that the relay models comply with the theory presented in the Section III.

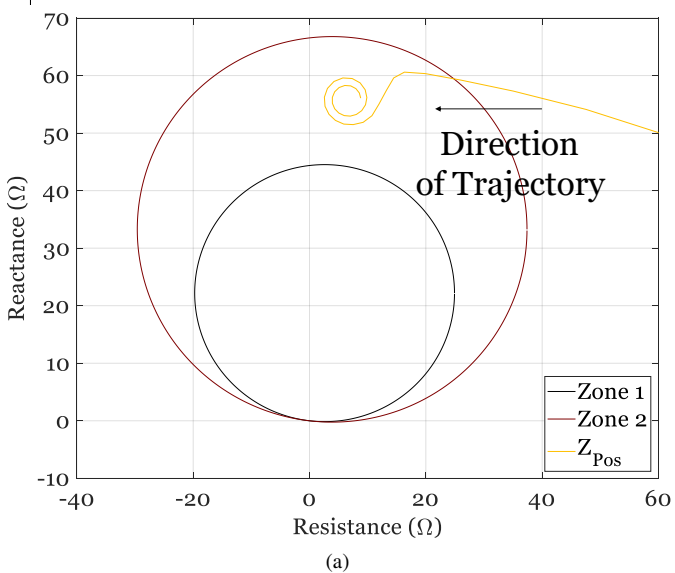
B. Simulation Results

Eight case studies are designed in this paper to evaluate the performance of distance relays at buses 8 and 9. Only L-G and line-to-line (L-L) faults are considered in this paper. The protection system worked correctly for five cases. However, it misoperated for three cases. These three test cases that exhibited results worthy of further analysis are reverse L-G fault at bus 9, forward L-L fault at bus 9, and reverse L-L at bus 8.

For the first case, the positive sequence impedance is conventional. However, the negative sequence value has an unconventional characteristic. A plot of the measured negative sequence impedance is given by Fig. 9. During the initial transients of the fault, the measured impedance rises sharply to the reverse area and then swings out beneath the forward threshold. It remains at this point for some time before returning again to the previous location. This is due to an extremely small magnitude negative sequence current being sourced by the DFIG, as well as a distorted wave pattern. If the reverse declaration is delayed longer than the intentional zone 2 delay, a trip signal is incorrectly issued for an out of zone fault.

The second case involves a forward L-L fault at bus 9. In this scenario the positive sequence impedance settles out in the fourth quadrant, extremely far from zone 1, as shown in Fig. 10. Due to the LVRT control structure, reactive power is injected to the grid during faults. This causes the measured impedance to be drastically different from the conventional value. Thus, the zone 1 element is not triggered in the relay. Since the fault is directly in front of the bus 9 relay, the protection should act instantaneously.

The reactive power injection affects fault sensing at the remote terminal as well. Case 3 presents a reverse L-L fault at the remote relay. Similarly to Case 2, there are errors in the measured positive sequence impedance. Fig. 11 shows the impedance trajectory crossing through the zone 1 element during the fault. The DFIG is unable to provide a significant amount of current at the remote bus so the measured impedance is incorrect, resulting in the trajectory shown in Fig.



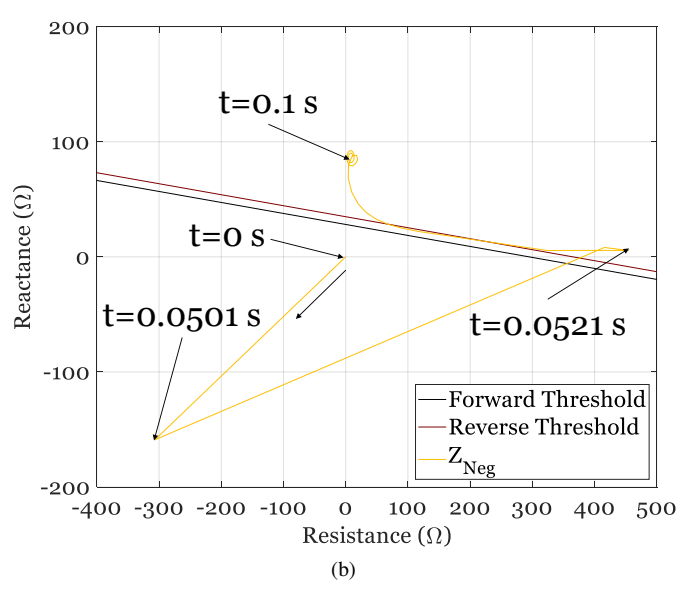


Fig. 8. Simulation results for a L-G fault at bus 8: (a) positive-sequence impedance trajectory measured at bus 9 and (b) negative-sequence impedance trajectory measured at bus 8.

11. These three cases represent situations where the protection response does not operate exactly as intended. If settings are not changed the protection may not detect faults correctly, putting the system at an increased risk of going unstable.

V. CONCLUSIONS

This paper studies the performance of distance relays protecting the line adjacent to a wind farm with Type III wind turbines. The wind turbines and relays are modeled in PSCAD/EMTDC software and their performance is tested on the IEEE 9-bus system. Simulation results demonstrate that distance relays may misoperate under circumstances that are imposed by the LVRT system of wind turbines, the negative sequence current sourced by the DFIGs, and their power electronics control system.

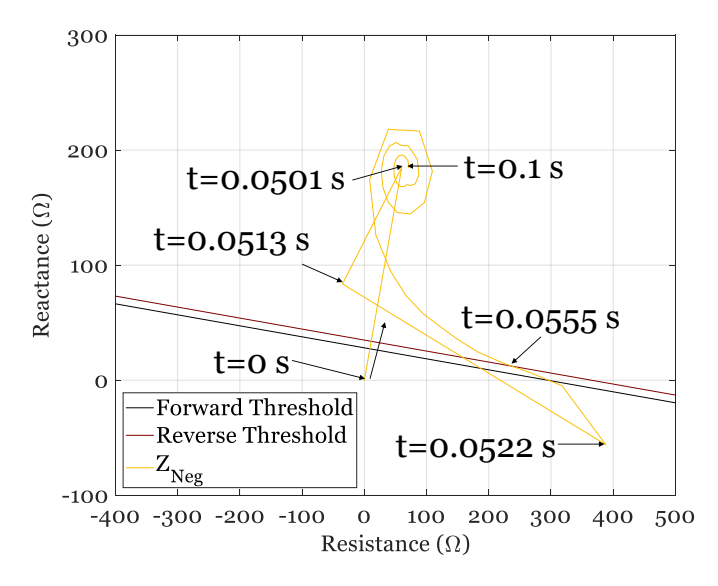


Fig. 9. Negative sequence impedance for reverse L-G fault at bus 9.

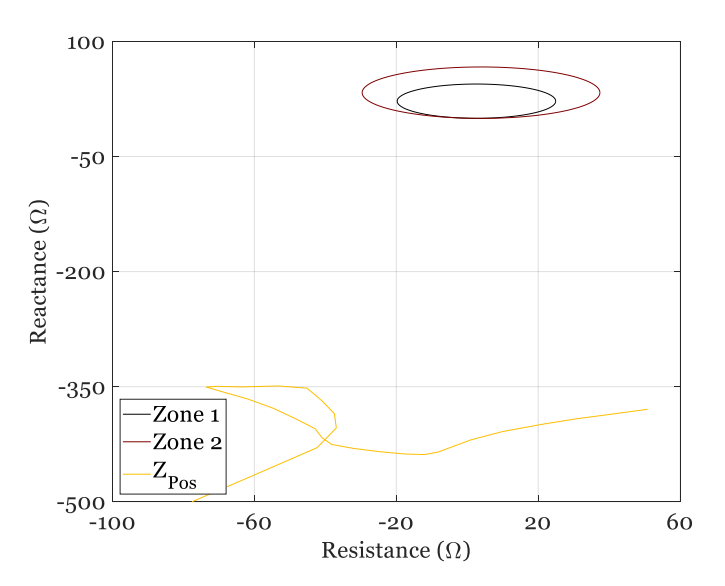


Fig. 10. Positive sequence impedance for forward L-L fault at bus 9.

REFERENCES

- [1] AWEA, "First Quarter 2020 Report," 2020. [Online]. Available: https://www.awea.org/resources/publications-and-reports/market-reports
- [2] S. Muller, M. Deicke, and R. W. De Doncker, "Doubly fed Induction Generator Systems for Wind Turbines," *IEEE Ind. Appl. Mag.*, vol. 8, no. 3, pp. 26–33, May 2002.
- [3] H. Ghaffarzdeh and A. Mehrizi-Sani, "Mitigation of Subsynchronous Resonance Induced by a Type III Wind System," *IEEE Trans. Sustain. Energy*, vol. 11, no. 3, pp. 1717–1727, Jul. 2020.
- [4] A. Mohammadhassani and A. Mehrizi-Sani, "A fault tolerant selective harmonic elimination method for modular multilevel converters," *IEEE Power Energy Soc. General Meeting*, Aug. 2020.
- [5] A. Mohammadhassani, A. Teymouri, A. Mehrizi-Sani, and K. Tehrani, "Performance evaluation of an inverter-based microgrid under cyberattacks," in *IEEE Int. Conf. Syst. Syst. Engr.*, Jun. 2020, pp. 211–216.
- [6] P. Sun, J. Yao, R. Liu, J. Pei, H. Zhang, and Y. Liu, "Virtual capacitance control for improving dynamic stability of the dfig-based wind turbines during a symmetrical fault in a weak ac grid," *IEEE Trans. Ind. Electron.*, vol. 68, no. 1, pp. 333–346, Jan. 2021.

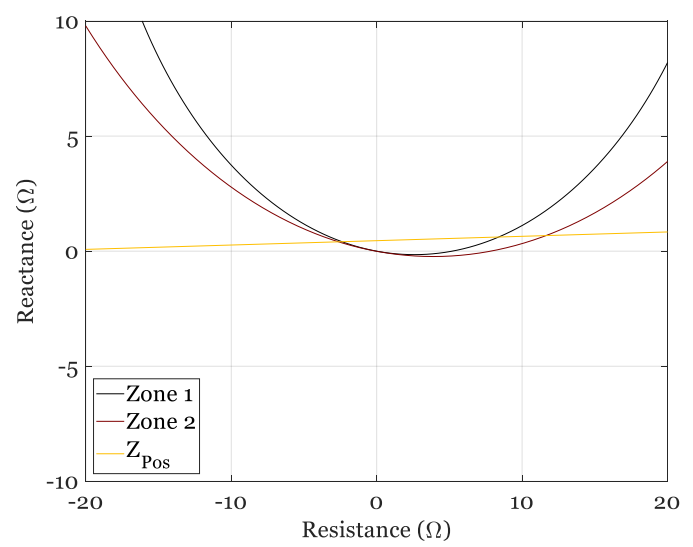


Fig. 11. Positive sequence impedance for reverse L-L fault at bus 8.

- [7] NERC, "Standard PRC-024-2: Generator Frequency and Voltage Protective Relay Settings," Jan. 2013. [Online]. Available: https://www.nerc.com/pa/Stand/Reliability%20Standards/PRC-024-2.pdf
- [8] S. Tohidi and B. Mohammadi-ivatloo, "A Comprehensive Review of Low Voltage Ride Through of Doubly Fed Induction Wind Generators," *Renew. and Sustain. Energy Reviews*, vol. 57, pp. 412–419, May 2016.
- [9] O. P. Mahela, N. Gupta, M. Khosravy, and N. Patel, "Comprehensive Overview of Low Voltage Ride Through Methods of Grid Integrated Wind Generator," *IEEE Access*, vol. 7, pp. 99299–99326, Jul. 2019.
- [10] A. Hooshyar, M. A. Azzouz, and E. F. El-Saadany, "Distance Protection of Lines Connected to Induction Generator-Based Wind Farms During Balanced Faults," *IEEE Trans. Sustain. Energy*, vol. 5, no. 4, pp. 1193– 1203, Oct. 2014.
- [11] M. Zolfaghari, R. M. Chabanlo, M. Abedi, and M. Shahidehpour, "A Robust Distance Protection Approach for Bulk AC Power System Considering the Effects of HVDC Interfaced Offshore Wind Units," *IEEE Syst. J.*, vol. 12, no. 4, pp. 3786–3795, Dec. 2018.
- [12] K. El-Arroudi and G. Joós, "Performance of Interconnection Protection Based on Distance Relaying for Wind Power Distributed Generation," *IEEE Trans. Power Del.*, vol. 33, no. 2, pp. 620–629, Apr. 2018.
- [13] S. Chen, N. Tai, C. Fan, J. Liu, and S. Hong, "Adaptive Distance Protection for Grounded Fault of Lines Connected with Doubly-Fed Induction Generators," *IET Gener. Transm.*, vol. 11, no. 6, pp. 1513– 1520, May 2017.
- [14] K. Zimmerman and D. Costello, "Fundamentals and Improvements for Directional Relays," in *Proc. 2010 63rd Annu. Conf. Protective Relay Engineers*, Mar. 2010, pp. 1–12.
- [15] Manitoba Hydro International Ltd., "Type 3 Wind Turbine Model," Nov. 2018. [Online]. Available: https://www.pscad.com/knowledge-base/article/496
- [16] Manitoba Hydro International Ltd., "IEEE 09 Bus System," May 2018.
 [Online]. Available: https://www.pscad.com/knowledge-base/article/25
- [17] H. Liu and Z. Chen, "Aggregated modelling for wind farms for power system transient stability studies," Asia-Pacific Power Energy Engr. Conf., pp. 1–6, Mar. 2012.